



# Synthesis of Novel Pyrimidin-4-One Bearing Piperazine Ring-Based Amides as Glycogen Synthase Kinase-3 $\beta$ Inhibitors with Antidepressant Activity

Imran Khan<sup>1</sup>, Mushtaq A. Tantray<sup>1</sup>, Hinna Hamid<sup>1,\*</sup>, Mohammad Sarwar Alam<sup>1</sup>, Abul Kalam<sup>2</sup>, Faraz Shaikh<sup>3</sup>, Anamik Shah<sup>3</sup> and Firasat Hussain<sup>4</sup>

<sup>1</sup>Department of Chemistry, Faculty of Science, Hamdard University, New Delhi 110 062, India

<sup>2</sup>Department of Pharmacology, Faculty of Pharmacy, Hamdard University, New Delhi 110 062, India

<sup>3</sup>National Facility for Drug Discovery, Department of Chemistry, Saurashtra University, Gujarat 360005, India

<sup>4</sup>Department of Chemistry, Faculty of Science, University of Delhi, New Delhi 110 062, India

\*Corresponding author: Hinna Hamid, hhamid@jamiahamdard.ac.in

Novel pyrimidin-4-one derivatives have been synthesized using EDC coupling and evaluated as glycogen synthase kinase-3 $\beta$  (GSK-3 $\beta$ ) inhibitors. Among all the synthesized compounds, compound 5 (3-methyl-6-phenyl-2-(piperazin-1-yl)-3,4-dihydropyrimidin-4-one) exhibited the most potent inhibitory activity against GSK-3 $\beta$  with IC<sub>50</sub> value of 74 nM. The molecular docking studies were performed to elucidate the binding modes of the compounds with the target, and a crucial interaction involving hydrogen bond formation with Val-135 to the active site of GSK-3 $\beta$  was observed. Furthermore, the synthesized compounds were subjected to in vivo evaluation of their antidepressant activity, and compound 5 showing highest inhibition of GSK-3 $\beta$  was also found to significantly reduce the duration of immobility at 50 mg/kg, when compared with fluoxetine, a known antidepressant drug. The results of our study suggest that compound 5 may serve as a valuable template for the design and development of inhibitors of GSK-3 $\beta$  with antidepressant activity.

**Key words:** antidepressant activity, EDC, glycogen synthase kinase-3 $\beta$ , molecular docking, piperazine, Pyrimidin-4-one

Received 11 July 2015, revised 23 September 2015 and accepted for publication 1 December 2015

Glycogen synthase kinase 3 (GSK-3) was one of the first kinases to be identified and initially studied for its function in the regulation of glycogen synthase. Glycogen synthase

kinase-3 (GSK-3) is a serine–threonine kinase that is involved in many physiological processes such as metabolism, cell-division cycle, apoptosis, transcription, neurotransmission, insulin action and gene expression (1). GSK-3 exists as two isoforms, GSK-3 $\alpha$  (51 kDa) and GSK-3 $\beta$  (47 kDa) sharing high homology in their kinase domains. Both isomers exist ubiquitously in cells and tissues and have similar biochemical properties. They differ significantly from one another outside N-terminal region, with GSK-3 $\alpha$  possessing an extended N-terminal glycine-rich tail (2). GSK-3 $\beta$  is the predominant isoform and phosphorylates tau proteins which regulate microtubule stability in neural cells. When dysregulated, GSK-3 $\beta$  can lead to the development of a wide variety of psychiatric and non-psychiatric human diseases, such as diabetes, cancer, inflammation, Alzheimer's disease, schizophrenia, attention deficit hyperactivity disorder (ADHD) and bipolar disorder. Among many diverse substrates, some of the key molecules mediating GSK-3 $\beta$  functions and regulating several cellular processes are glycogen synthase (GS), tau protein and beta catenin proteins (3). GSK-3 $\beta$ -specific inhibitors might be thus promising and effective drugs for the treatment of devastating pathologies such as neurodegenerative diseases, stroke and mood disorders (4). In Alzheimer's disease (AD), a neurodegenerative disorder defined by progressive memory loss and cognitive impairment, the presence of toxic aggregates is formed in the brain such as extracellular amyloid deposits (accumulation of  $\beta$ -amyloid peptides) and intracellular neurofibrillary tangles that result from the misfolding of hyperphosphorylated tau protein. Tau is a microtubule-associated protein which promotes the assembly and stabilization of microtubules in neurons (5). GSK-3 $\beta$  has been found to be the prime suspect responsible for post-translational aberrant modifications of tau protein (6).

Diverse chemotypes of GSK-3 $\beta$  inhibitors have been reported and reviewed in the literature. Lithium is the first known inhibitor against GSK-3 $\beta$  which inhibits GSK-3 $\beta$  directly and indirectly. Lithium is indicated as a preferential treatment for bipolar disorders, and the ability of this cation to inhibit GSK-3 $\beta$  has been proposed as a potential mechanism of action (7–9). GSK-3 $\beta$  has been implicated in the mechanism of action of the mood stabilizers lithium and valproate, (10,11) largely used in the treatment of bipolar disorder (12). Furthermore, dysfunctional GSK-3 $\beta$  has also been found to be involved in major depression (13). This

involvement could be linked to the deficient serotonergic neurotransmission observed in depression (14), considering that serotonergic activity contributes to the inhibitory control of GSK-3 $\beta$  in mammalian brain *in vivo* (15). This conclusion is based on the finding that serotonin (5-HT) itself, as well as fluoxetine (a selective serotonin re-uptake inhibitor) and 5-HT<sub>1A</sub> agonists, augments serine 9 phosphorylation with the consequent inhibition of GSK-3 $\beta$  (15). There have been several reports demonstrating that pharmacologic inhibition of GSK-3 activity produces antidepressant-like effects in rodents (16).

Small molecule GSK-3 $\beta$  inhibitors based on scaffolds such as oxadiazoles, oxazoles, thiazolidinones, thiazoles, pyrimidines, pyrimidones, benzimidazoles, purines, pyrazolopyrimidines, furopyrimidines, indirubins and paulinones have also been reported (17–29). Pyrimidine/pyrimidin-4-one has been illustrated as one of the best scaffolds for GSK-3 (21,30) and cancer inhibition (31,32). The recently launched kinase inhibitor drugs Dasatinib and Pazopanib, which are pyrimidine derivatives, inhibit a broad array of cancer-related protein kinases.

Piperazine moiety is considered to be a privileged ligand in drug discovery and is present in several bio-active molecules of many therapeutic areas, viz. antibacterial, anticonvulsant, antidepressant, anticancer and antidiabetic (33–37). Hence, this work was carried out with an objective to develop some novel piperazine conjugates of pyrimidones as GSK-3 inhibitors and to explore the effect of other similar secondary amines on GSK-3 inhibition of pyrimidone scaffold (Figure 1).

Along these lines, compounds showing promising GSK-3 $\beta$  inhibitory activity were also evaluated for their antidepressant activity.

## Materials and Methods

### Drug and reagents

Human recombinant glycogen synthase kinase-3 $\beta$  and prephosphorylated polypeptide substrate GS-2 were purchased from Merck-Millipore Corporation (New Delhi, India). Kinase-Glo Luminescent Kinase Assay (catalog number V6713) was obtained from Promega Corporation (Madison, WI, USA). Staurosporine and ATP were purchased from Sigma-Aldrich (Bangalore, Karnataka, India).

Glow-type luminescence was recorded on Infinite F200<sup>®</sup> PRO (Tecan, Tecan Group Ltd., Switzerland) instrument. Fluoxetine hydrochloride was purchased from local market. All commercial chemicals used as starting materials and reagents were of analytical grade and purchased from Merck (New Delhi, India), Spectrochem and Sigma-Aldrich. All melting points are uncorrected and have been measured using Veego VMP-DS apparatus. IR spectra were recorded as KBr pellets on a Perkin Elmer 1650 spectrophotometer (Perkin Elmer, Inc., Waltham, MA, USA). <sup>1</sup>H NMR spectra were determined on a Bruker (300 or 400 MHz) spectrometer (Bruker BioSpin AG Fallanden, Switzerland), and chemical shifts are expressed as ppm against TMS as internal reference. Mass spectra were recorded on 70 eV (EI Ms-QP 1000EX, Shimadzu, Japan). Column chromatography was performed on silica gel (60–120 mesh). Elemental analysis was carried out using Elementar Vario EL III elemental analyser (Elementar Analysensysteme, Hanau, Germany). Elemental analysis data is reported in percentage standard. The compounds were synthesized using 1-(3-dimethylaminopropyl)-3-ethylcarbodiimide hydrochloride (EDC) coupling (Scheme 1).

### General procedure for synthesis of 2-mercapto-3,4-dihydropyrimidin-4-one

$\beta$ -Ketoester (10 g, 52.08 mmol) was dissolved in ethanol (50 mL) containing N-methyl thiourea (7.03 g, 78.12 mmol) and DBU (7.91 g, 52.08 mmol). The reaction mixture was refluxed and stirred for 8 h. The progress of the reaction was monitored by TLC. After completion, the reaction mixture was concentrated and cooled. After cooling, the reaction mixture was added slowly to a solution of water methanesulphonic acid (90:10) to get a thick precipitate, which was filtered and washed with water. The product obtained was then recrystallized from ethanol.

### General procedure for synthesis of 2-(methylthio)-3,4-dihydropyrimidin-4-one

2-mercapto-3,4-pyrimidin-4-one (8.5 g, 38.99 mmol) derivative was dissolved in dry DMF (50 mL). Methyl iodide (8.24 g, 58.07 mmol) and K<sub>2</sub>CO<sub>3</sub> (10.76 g, 77.98 mmol) were added followed by stirring for 12 h at room temperature. The progress of the reaction was monitored by TLC. After the completion of the reaction, the reaction mixture was poured onto ice-cooled water to get a precipitate. The precipitate was filtered and dried to obtain pure product.

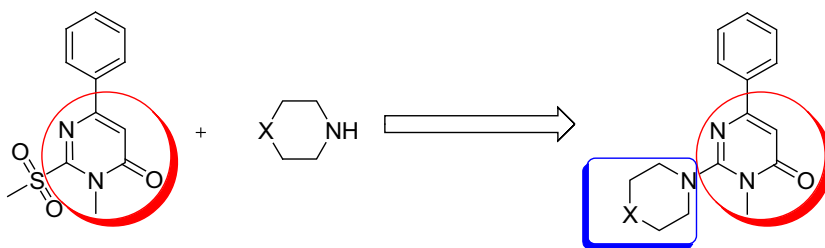
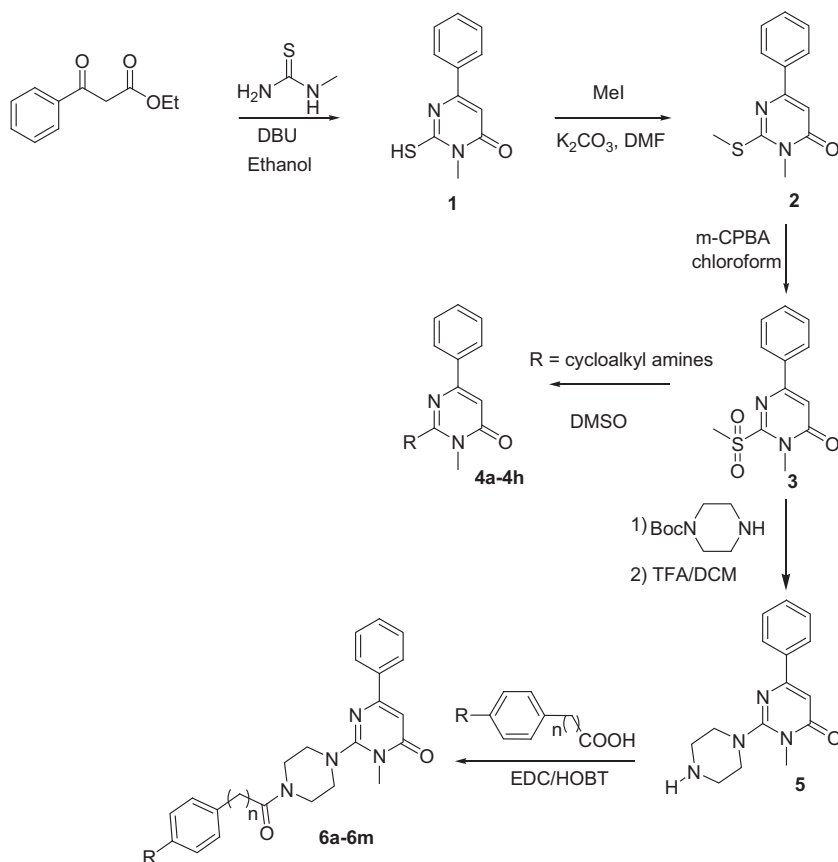


**Figure 1:** Chemotype structure.



**Scheme 1:** Synthesis of novel piperazinyl pyrimidin-4-one derivatives.

### General procedure for synthesis of 2-(methylthio)-3,4-dihydropyrimidin-4-one

2-(methylthio)-3,4-pyrimidin-4-one (7.0 g, 30.17 mmol) derivative was dissolved in chloroform (80 mL) and fresh 3-chloro perbenzoic acid (m-CPBA) (12.97 g, 75.43 mmol) added in three portions. The reaction mixture was allowed to stir at room temperature for 4 h. After completion of the reaction, as monitored by TLC, reaction mixture was quenched with water and the organic layer was separated. Combined organic layers were dried over anhydrous sodium sulphate, filtered and concentrated under reduced pressure to obtain the required product.

### General procedure for synthesis of piperazinyl-3,4-dihydropyrimidin-4-one derivatives

2-(methylsulfonyl)-3,4-pyrimidin-4-one (5 g, 18.93 mmol) derivative was treated with N-Boc piperazine (3.52 g, 18.93 mmol) or other secondary amines in DMSO (25 mL) to obtain different conjugates. In case of N-Boc piperazinyl-3,4-pyrimidin-4-one, the Boc protection was removed using 50% TFA in chloroform. The progress of the reaction was monitored by TLC. After completion of the reaction, reaction mixture was concentrated and subjected to purification by column chromatography to obtain the pure product.

### General procedure for synthesis of piperazinyl-3,4-dihydropyrimidin-4-one amide derivatives

Different aryl/benzyl carboxylic acids (200 mg, 1.63 mmol) were dissolved in dry DMF (5 mL), and HOBT (catalytic amount) was added followed by stirring for 15 min at room temperature. 2-piperazinyl-3,4-pyrimidin-4-one (442 mg, 1.63 mmol) was then added to the reaction mixture followed by addition of EDC.HCl (468 mg, 2.44 mmol) after 20 min. The reaction mixture was allowed to stir for 8–10 h. The reaction was monitored by TLC. After completion, the reaction mixture was poured onto crushed ice and extracted with ethyl acetate. The combined organic layers were dried over anhydrous sodium sulphate, concentrated and purified by column chromatography.

### Pharmacology

The investigations were carried out on swiss albino mice (35–45 g). The mice were procured from Central Animal House, Hamdard University, New Delhi. The animals were kept in cages at the room temperature and fed with food and water *ad libitum*. The experiments were performed in accordance with the rules of Institutional Animals Ethics Committee. The doses indicated are for the salt form used. All compounds administered orally were either suspended in 0.5% methylcellulose (Methocel) or dissolved in



distilled water when soluble and applied in a volume of 10 mL/kg, 1 h before behavioural testing.

### GSK-3 $\beta$ activity assay

Evaluation of GSK-3 $\beta$  inhibition activity of the synthesized compounds was performed in assay buffer using black 96-well plates according to the Kinase-Glo assay method of Baki<sup>28</sup> (38). In a typical assay, 10  $\mu$ L of test compound of different concentrations (dissolved in dimethyl sulphoxide [DMSO] and diluted with assay buffer) and 10  $\mu$ L (20 ng) of enzyme were added to each well followed by 20  $\mu$ L of assay buffer containing 25  $\mu$ M substrate, that is, glycogen synthase-2 and 1  $\mu$ M ATP. The final DMSO concentration in the reaction mixture was less than 1%. After incubation at 30 °C for 30 min, the enzymatic reaction was quenched with 40  $\mu$ L of Kinase-Glo reagent. Luminescence was recorded after 10 min using Infinite F200<sup>®</sup> PRO multimode reader (Tecan). The activity is proportional to the difference of the total and consumed ATP. The inhibitory activities were calculated on the basis of maximal activities measured in the absence of inhibitor. The IC<sub>50</sub> value was defined as the concentration of each compound that reduces 50% the enzymatic activity with respect to that without inhibitors. Staurosporine was used as a positive control for evaluation of GSK3 $\beta$  inhibition.

### Antidepressant activity

#### Tail suspension test (TST)

The tail suspension test as a model of behavioural despair was carried out according to the method reported by Vincent Castagne and co-workers's method (39). Mice were moved from the housing colony room to the testing laboratory and stayed undisturbed for at least 1 h before testing. Mice were suspended by the tail using adhesive scotch tape, to a hook connected to a strain gauge that picked up all the movements of the mouse and transmitted them to a central unit that calculated the total duration of immobility during a 6-min test with the help of a MAZE software version 3.0. (Stoelting Co., Wood Dale, IL, USA) Data collected were expressed as a mean of immobility time (in second  $\pm$  the standard error mean: SEM).

#### Forced swim test

The forced swim test (FST) or despair swim test has been proposed as model to test for antidepressant activity by Vincent Castagne and co-workers's method (39). Mice were moved from the housing colony room to the testing laboratory where mice stayed undisturbed for at least 1 h before testing. They were provided free access to standard rodent diet and tap water, and a controlled temperature of 21°  $\pm$  3 °C and standard light/dark cycle with illumination from 0700 to 1900 was maintained. They were administered appropriate treatment at 50 mg/kg dose, and the test was started 1 h post-administration. Each

mouse was placed for six minutes in a cylindrical tank (height, 25 cm; diameter, 15 cm) containing 20 cm of water maintained at 25  $\pm$  1 °C. Duration of immobility, defined as lack of activity, except movements made by mice to keep their heads above water, was scored during the last four minutes. Data was compared with the data from the control and the standard group.

### Molecular modelling studies

All the molecules were docked against (PDB ID: 1Q3W) GSK-3 $\beta$  complex using Glide module of Schrodinger. Preceding to docking by GLIDE, preparation wizard of Mastero's GUI interface was used for protein structure preparation (40). The minimization was implemented using OPLS force field taking implicit solvation (41). Ligprep included with Schrodinger software was used for preparation of all ligands (42). Active site radius was taken as 12.0 Å so that the active site residues namely ASP133, VAL135, ARG141, ASP200, CYS199, LEU132, GLU185, GLU97, LYS85 and PHE67 could be included. The prepared protein and Ligprep generated prepared ligands were further subjected to extra precision (XP Docking) by taking Glide module via Maestro interface (41). The Glide takes systematic sampling approach, which considers ligand's position, conformation and alignment before estimating the energy between the ligand-protein interaction. Following calculation was used to generate Gscore by Glide (43, 44).

$$\text{G-score} = 0.05 * \text{vdW} + 0.15 * \text{Coul.} + \text{Lipo} + \text{H-bond} + \text{Metal} + \text{Rewards} + \text{RotB} + \text{Site.}$$

The docked protein-ligand complex was ranked by GLIDE's Gscore and Prime MM/GBSA-based rescoring.

## Results and Discussion

### Chemistry

$\beta$ -Keto ester and N-substituted thiourea were refluxed in dry methanol using 1,8-diazabicyclo(5,4,0) undec-7-ene (DBU) as base to form thiopyrimidone **1** which was treated with methyl iodide in the presence of potassium carbonate in dry N,N-dimethyl formamide (DMF) to form methyl thiopyrimidone **2**. The methyl thiopyrimidone was oxidized to methyl sulphonyl pyrimidone **3** with m-chloroperbenzoic acid in dry chloroform at room temperature. Mesityl group was nucleophilically substituted with various cyclic secondary amines viz. 2-methyl piperidine, piperidine, 4-amino morpholine, 4-methyl piperazine, morpholine, thiomorpholine, pyrrolidine and N-Boc piperazine in order to attain the corresponding compounds **4a-4g**. Furthermore, compound **4h** obtained from the nucleophilic substitution with N-Boc piperazine was directly used in the next step without purification and N-Boc was deprotected by stirring in 50% TFA in chloroform to obtain 2-piperazinyl pyrimidone **5**. The 2-piperazinyl pyrimidone compound **5** was then

coupled with various substituted aryl and benzyl carboxylic acids using 1-(3-dimethylaminopropyl)-3-ethylcarbodiimide hydrochloride (EDC) coupling to obtain the target molecules **4a-g**, **5**, **6a-m** (Scheme 1) (45). A focused library of 21 compounds was synthesized Table S1 and Table S2, and all the synthesized compounds were screened for their GSK-3 $\beta$  inhibitory activity.

The formation of the thiopyrimidone intermediate was confirmed by the presence of signals at  $\delta$  6.22 (s, 1H, CH for proton of pyrimidin-4-one ring) and 12.73 (s, 1H, SH for proton of thiol group). Attachment to the cyclic secondary amines was confirmed by the appearance of the corresponding methylene protons in the  $^1\text{H-NMR}$  spectra, for example, in case of piperazine – two multiplets appeared at  $\delta$  3.34–3.36 (m, 4H, CH<sub>2</sub>) and  $\delta$  3.53–3.55 (m, 4H, CH<sub>2</sub>). Furthermore,  $^1\text{H-NMR}$  spectra also showed the presence of the aryl protons indicating the formation of amide bond to aryl and benzyl carboxylic acids in case of piperazine analogues. The structure was further supported by the  $^{13}\text{C-NMR}$  and mass spectra. ESI-MS of all compounds showed  $[\text{M}]^+$ ,  $[\text{M} + 1]^+$  and  $[\text{M} + 2]^+$  peaks.

### In vitro GSK-3 $\beta$ inhibition

All the synthesized compounds were evaluated for GSK-3 $\beta$  inhibitory activity in a non-radioactive assay using Kinase-Glo reagents, and the results are shown in Table S1 and Table S2.

Staurosporine, a well-known kinase inhibitor, was used as the reference compound. The test compounds were first screened at a primary concentration of 10  $\mu\text{M}$ . Compounds showing less than 50% inhibition were considered as inactive ( $\text{IC}_{50} > 10 \mu\text{M}$ ). Compounds displaying more than 50% inhibition at 10  $\mu\text{M}$  were next tested over a wide range of concentrations, and  $\text{IC}_{50}$  values were determined from the dose-response curves.

The results of kinase inhibitory assays demonstrated that compound **5** was the most potent among the cyclic secondary amine-pyrimidone conjugates with  $\text{IC}_{50}$  value of 74 nM. Among the amide conjugates of compound **5**, compounds **6b**, **6c**, **6f** and **6j** showed significant inhibitory potency against GSK-3 $\beta$  with  $\text{IC}_{50}$  values 127, 116, 83, 89 nM, respectively.

### In vivo antidepressant activity

#### Tail suspension test (TST)

The results as depicted in Figure 2 show the effect of immobility in the tail suspension test. The mean duration of immobility was significantly reduced in standard drug fluoxetine shows immobility time of 227 seconds, and test compounds **5**, **6f**, **6j**, **6c**, **6b** show immobility time of 187, 197, 196, 206, 217 seconds as compared to the normal saline immobility time of 234 seconds ( $p < 0.05$ ). Decrease in immobility time with test compounds was statistically significant except in **6b** when compared with normal saline, whereas **5**, **6f**, **6j** also showed significant decrease in comparison with the standard drug fluoxetine.

#### Forced swim test

The effect of immobility in the forced swim test results is shown in the Figure 3. Significantly, decreases in immobility time were observed during the test in all the compounds (**5**, **6f**, **6j**, **6c**, **6b**) compared with normal saline ( $p < 0.05$ ). While as the compounds **5** and **6f** were also found to exhibit significant activity compared with the standard drug fluoxetine.

### Molecular modelling studies

Synthesized piperazinyl pyrimidin-4-one derivatives were subjected to docking calculations using Glide score to study the docking results (Table S3 and Figure 4). Based

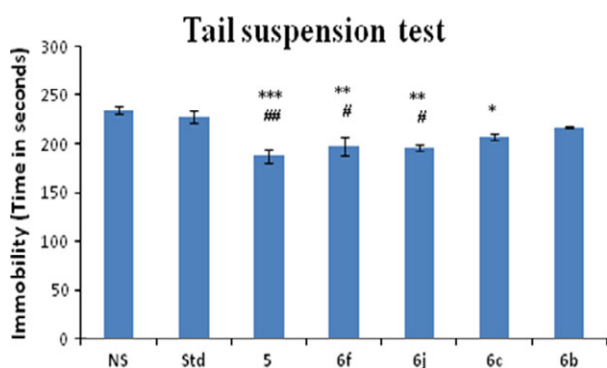


**Figure 2:** Tail suspension test. Data is represented as mean  $\pm$  SEM and analysed by one-way ANOVA followed by Tukey-Kramer multiple comparison test, \* $p < 0.05$ , \*\* $p < 0.01$ , \*\*\* $p < 0.001$ , # $p < 0.05$ , ## $p < 0.01$ , ### $p < 0.001$  when compared with normal control and standard (fluoxetine), respectively.

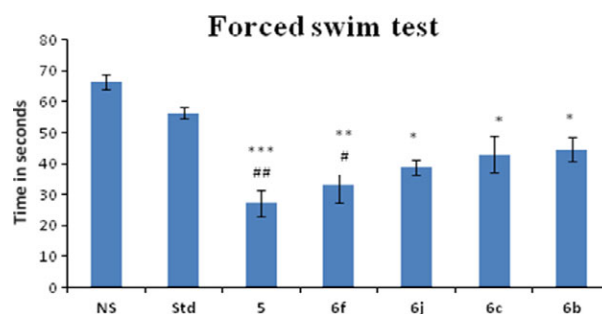


**Figure 3:** Forced swim test. Data is represented as mean  $\pm$  SEM and analysed by one-way ANOVA followed by Tukey-Kramer multiple comparison test, \* $p < 0.05$ , \*\* $p < 0.01$ , \*\*\* $p < 0.001$ , # $p < 0.05$ , ## $p < 0.01$ , ### $p < 0.001$  when compared with normal control and standard (fluoxetine), respectively.

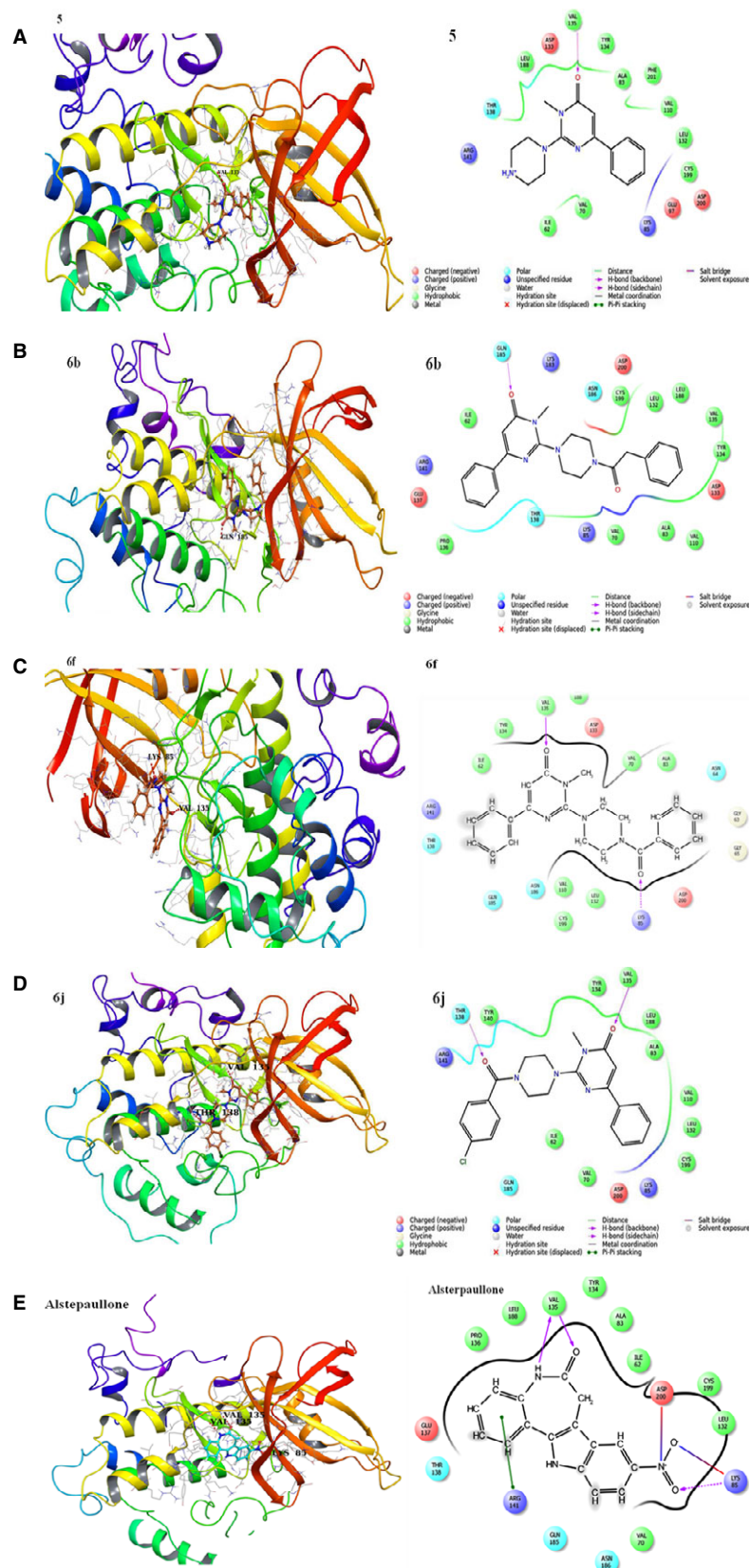


**Figure 4:** (A) Ligand–protein interaction map provides insight into the detail of compound **5**. (B) Ligand–protein interaction map provides insight into the detail of compound **6b**. (C) Ligand–protein interaction map provides insight into the detail of compound **6f**. (D) Ligand–protein Interaction map provides insight into the detail of compound **6j**. (E) Ligand–protein Interaction map provides insight into the detail of standard ligand.

on 'Glide G-score', it has been found that among the synthesized compounds **6f** has significant binding affinity towards GSK-3 $\beta$ , which shows two hydrogen bond interactions with Val135 and Lys85 with a G-score of  $-6.573$ . The ligands **6j** and **6b** bind with a G-score of  $-6.467$  and  $-6.364$ , respectively, and a Prime MMGBSA value of  $-46.693$  and  $-61.681$ , and they interact by forming hydrogen bonds with crucial residues such as Val135, Thr138 and G185. Compound **5**, exhibiting a G-score of  $-5.962$ , shows a hydrogen bond interaction with Val135. The results of the *in silico* studies were found to be in agreement with the *in vitro* GSK-3 assay as the 4 top-ranked ligands (**6f**, **6j**, **6b** and **5**) which showed better binding affinity in *in silico* studies also exhibited highest *in vitro* activity.

From the results obtained, inhibition of GSK-3 $\beta$  was found to increase in accordance with the following changes made in the structure of the synthesized compounds (Scheme 2).

### Crystallographic study

Intensity data were collected at 183(2) K an Oxford Xcalibur Sapphire 3 diffractometer (a single wavelength enhance X-ray source with MoK $\alpha$  radiation,  $\lambda = 0.71073$  Å) (46). The selected suitable single crystal was mounted using paratone oil on the top of a glass fibre fixed on a goniometer head and immediately transferred to the diffractometer. Pre-experiment, data collection, data reduction and analytical absorption corrections (46,47) were performed with the Oxford program suite *CrysAlisPro* (48). The crystal structures were solved with SHELXS-97 (48) using direct methods. The structure refinements were performed by full-matrix least-squares on  $F^2$  with SHELXL-97 (48). All programs used during the crystal structure determination process are included in the WINGX software (48).

The chemical formula and ring labelling system is shown in Figure 5. Crystal data for compound **6g**: C $_{23}$ H $_{24}$ N $_4$ O $_2$ , molecular weight, 388.46; system, monoclinic; space

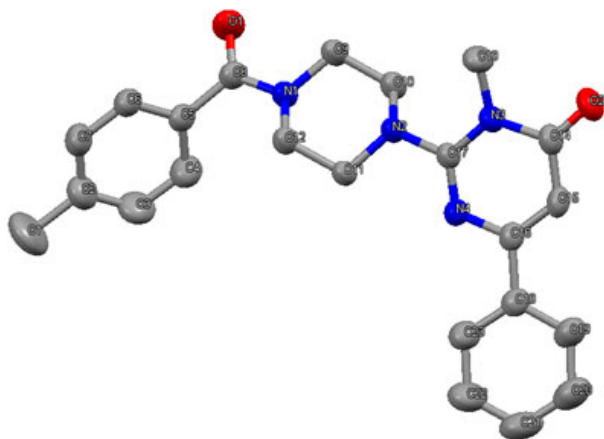
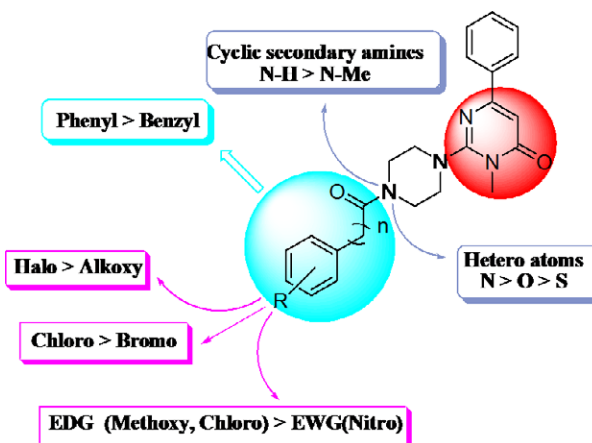


**Figure 5:** Crystal structure of **6j**.



**Scheme 2:** Structure Activity Relationship

group, P 21/c; unit cell dimensions,  $a = 15.0557(11)$  Å;  $b = 15.3211(10)$  Å;  $c = 8.9228(7)$  Å;  $\beta = 95.789(7)^\circ$ ;  $V = 2047.7(3)$  Å $^3$ ;  $Z = 2$ ;  $T = 298$  K;  $R_{int} = 0.0524$ ;  $R(all) = 0.1284$ ;  $Gof = 1.018$ ;  $\Delta\rho_{max} = 0.195$  e Å $^{-3}$ ;  $\Delta\rho_{min} = -0.192$  e Å $^{-3}$ . The resolution obtained for the structure of the compounds was limited by the poor quality of the available crystals.

All hydrogen atoms were calculated after each cycle of refinement using a riding model, with C-H =  $0.93$  Å +  $U_{iso}(H) = 1.2U_{eq}(C)$  for aromatic H atoms, with C-H =  $0.97$  Å +  $U_{iso}(H) = 1.2U_{eq}(C)$  for methylene H atoms.

Crystallographic data for the structure **6g** has been deposited with the Cambridge Crystallographic Data Center (CCDC) under the number CCDC 1401787.

### Conclusion

A focussed library of piperazinyl pyrimidin-4-one derivatives was evaluated for GSK-3 $\beta$  inhibitory activity, and an SAR has been drawn based on the study. Among the tested compounds, piperazine conjugate **5** was found to be the most active ( $IC_{50} = 74$  nM) while N-benzoylated/N-acylated conjugates (**6b**, **6c**, **6f**, **6j**) of **5** exhibited activity comparable to compound **5**. Furthermore, *in vivo* antidepressant activity was evaluated by two behavioural models, viz. tail suspension test (TST) and forced swim test (FST). Tail suspension test and forced swim test showed that compound **5** significantly reduced the duration of immobility at 50 mg/kg, when compared with the normal saline and standard drug ( $p < 0.05$ ).

### Acknowledgments

The authors wish to express their thanks to Dr. G. N. Qazi, Vice Chancellor, Jamia Hamdard for providing necessary

facilities to carry out this work. The authors thank DST-SERB, Govt. of India, for awarding research project to HH and fellowship to IK.

## References

1. Sperbera B.R., Leight S., Goedert M., Lee V.M.Y. (1995) Glycogen synthase kinase-3 $\beta$  phosphorylates tau protein at multiple sites in intact cells. *Neurosci Lett*;197:149–153.
2. Woodgett J. (1990) Molecular cloning and expression of glycogen synthase kinase-3/factor A. *EMBO J*;9:2431–2438.
3. Cohen P., Frame S. (2001) The renaissance of GSK3. *Nat Rev Mol Cell Biol*;2:769–776.
4. Palomo V., Perez D.I., Perez C., Morales-Garcia J.A., Soteras I., Alonso-Gil S. *et al.* (2012) 5-imino-1,2,4-thiadiazoles: first small molecules as substrate competitive inhibitors of glycogen synthase kinase 3. *J Med Chem*;55:1645–1661.
5. Mazanetz M.P., Fischer P.M. (2007) Untangling tau hyperphosphorylation in drug design for neurodegenerative diseases. *Nat Rev Drug Discovery*;6:464–479.
6. Blennow K., de Leon M.J., Zetterberg H. (2006) Alzheimer's disease. *Lancet*;368:387–403.
7. Klein P.S., Melton D.A. (1996) A molecular mechanism for the effect of lithium on development. *Proc Natl Acad Sci USA*;93:8455–8459.
8. Phiel C.J., Klein P.S. (2001) Molecular targets of lithium action. *Annu Rev Pharmacol Toxicol*;41:789–813.
9. Jope R.S. (2003) Lithium and GSK-3: one inhibitor, two inhibitory actions, multiple outcomes. *Trends Pharmacol Sci*;24:441–443.
10. Chen G., Huang L.D., Jiang Y.M., Manji H.K. (1999) The mood-stabilizing agent valproate inhibits the activity of glycogen synthase kinase-3. *J Neurochem*;72:1327–1330.
11. Li X., Bijur G.N., Jope R.S. (2002) Glycogen synthase kinase-3 $\beta$ , mood stabilizers, and neuroprotection. *Bipolar Disord*;4:137–144.
12. Jope R.S. (1999) Anti-bipolar therapy: mechanism of action of lithium. *Mol Psychiatry*;4:117–128.
13. Jope R.S., Roh M.-S. (2006) Glycogen Synthase Kinase-3 (GSK3) in psychiatric diseases and therapeutic interventions. *Curr Drug Targets*;7:1421–1434.
14. Berns G.S., Nemeroff C.B., editors. (2003) *The Neurobiology of Bipolar Disorder*. American Journal of Medical Genetics Part C: Seminars in Medical Genetics. 123C: Wiley Online Library (UK); 76–84 p.
15. Li X., Zhu W., Roh M.S., Friedman A.B., Rosborough K., Jope R.S. (2004) In vivo regulation of glycogen synthase kinase-3 $\beta$  (GSK3 $\beta$ ) by serotonergic activity in mouse brain. *Neuropsychopharmacology*;29:1426–1431.
16. Gould T.D., Zarate C.A., Manji H.K. (2004) Glycogen synthase kinase-3: a target for novel bipolar disorder treatments. *J Clin Psychiatry*;65:10–21.
17. Saitoh M., Kunitomo J., Kimura E., Hayase Y., Kobayashi H., Uchiyama N. *et al.* (2009) Design, synthesis and structure-activity relationships of 1,3,4-oxadiazole derivatives as novel inhibitors of glycogen synthase kinase-3 $\beta$ . *Bioorg Med Chem*;17:2017–2029.
18. Saitoh M., Kunitomo J., Kimura E., Iwashita H., Uno Y., Onishi T. *et al.* (2009) 2-{3-[4-(Alkylsulfonyl)phenyl]-1-benzofuran-5-yl}-5-methyl-1,3,4-oxadiazole derivatives as novel inhibitors of glycogen synthase kinase-3 $\beta$  with good brain permeability. *J Med Chem*;52:6270–6286.
19. Ring D.B., Johnson K.W., Henriksen E.J., Nuss J.M., Goff D., Kinnick T.R. *et al.* (2003) Selective glycogen synthase kinase 3 inhibitors potentiate insulin activation of glucose transport and utilization in vitro and in vivo. *Diabetes*;52:588–595.
20. Gentile G., Merlo G., Pozzan A., Bernasconi G., Bax B., Bamborough P. *et al.* (2012) 5-Aryl-4-carboxamide-1,3-oxazoles: potent and selective GSK-3 inhibitors. *Bioorg Med Chem Lett*;22:1989–1994.
21. Martinez A., Alonso M., Castro A., Perez C., Moreno F.J. (2002) First non-ATP competitive glycogen synthase kinase 3  $\beta$  (GSK-3 $\beta$ ) inhibitors: thiazolidinones (TDZD) as potential drugs for the treatment of Alzheimer's disease. *J Med Chem*;45:1292–1299.
22. Bhat R., Xue Y., Berg S., Hellberg S., Ormo M., Nilsson Y. *et al.* (2003) Structural insights and biological effects of glycogen synthase kinase 3-specific inhibitor AR-A014418. *J Biol Chem*;278:45937–45945.
23. Uehara F., Shoda A., Aritomo K., Fukunaga K., Watanabe K., Ando R. *et al.* (2013) 6-(4-Pyridyl)pyrimidin-4 (3H)-ones as CNS penetrant glycogen synthase kinase-3 $\beta$  inhibitors. *Bioorg Med Chem Lett*;23:6928–6932.
24. Lee S.C., Shin D., Cho J.M., Ro S., Suh Y.G. (2012) Structure-activity relationship of the 7-hydroxy benzimidazole analogs as glycogen synthase kinase 3 $\beta$  inhibitor. *Bioorg Med Chem Lett*;22:1891–1894.
25. Ibrahim N., Mouawad L., Legraverend M. (2010) Novel 8-arylated purines as inhibitors of glycogen synthase kinase. *Eur J Med Chem*;45:3389–3393.
26. Peat A.J., Boucheron J.A., Dickerson S.H., Garrido D., Mills W., Peckham J. *et al.* (2004) Novel pyrazolopyrimidine derivatives as GSK-3 inhibitors. *Bioorg Med Chem Lett*;14:2121–2125.
27. Miyazaki Y., Maeda Y., Sato H., Nakano M., Mellor G.W. (2008) Rational design of 4-amino-5,6-diaryl-furo [2,3-d]pyrimidines as potent glycogen synthase kinase-3 inhibitors. *Bioorg Med Chem Lett*;18:1967–1971.
28. Polychronopoulos P., Magiatis P., Skaltsounis A.L., Myrianthopoulos V., Mikros E., Tarricone A. *et al.* (2004) Structural basis for the synthesis of indirubins as potent and selective inhibitors of glycogen synthase kinase-3 and cyclin-dependent kinases. *J Med Chem*;47:935–946.
29. Leost M., Schultz C., Link A., Wu Y.Z., Biernat J., Mandelkow E.M. *et al.* (2000) Paullones are potent inhibitors of glycogen synthase kinase-3 $\beta$  and

- cyclin-dependent kinase 5/p25. *Eur J Biochem*; 267:5983–5994.
30. McCormack P.L., Keam S.J. (2011) Dasatinib: a review of its use in the treatment of chronic myeloid leukaemia and Philadelphia chromosome-positive acute lymphoblastic leukaemia. *Drugs*;71:1771–1795.
  31. Fukunaga K., Sakai D., Watanabe K., Nakayama K., Kohara T., Tanaka H. *et al.* (2015) Discovery of novel 2-(alkylmorpholin-4-yl)-6-(3-fluoropyridin-4-yl)-pyrimidin-4(3H)-ones as orally-active GSK-3 $\beta$  inhibitors for Alzheimer's disease. *Bioorg Med Chem Lett*;25:1086–1091.
  32. Nieto M., Borregaard J., Ersboll J., ten Bosch G.J., van Zwieten-Boot B., Abadie E. *et al.* (2011) The European Medicines Agency review of pazopanib for the treatment of advanced renal cell carcinoma: summary of the scientific assessment of the Committee for Medicinal Products for Human Use. *Clin Cancer Res*;17:6608–6614.
  33. Appelbaum P.C., Hunter P.A. (2000) The fluoroquinolone antibacterials: past, present and future perspectives. *Int J Antimicrob Agents*;16:5–15.
  34. Marona H., Korona R., Szneler E. (2004) Synthesis and anticonvulsant activity of some piperazine derivatives. *Boll Chim Farm*;143:329–335.
  35. Lee Y.B., Gong Y.D., Yoon H., Ahn C.H., Jeon M.K., Kong J.Y. (2010) Synthesis and anticancer activity of new 1-[(5 or 6-substituted 2-alkoxyquinoxalin-3-yl)aminocarbonyl]-4-(hetero)arylpiperazine derivatives. *Bioorg Med Chem*;18:7966–7974.
  36. Seo H.J., Park E.-J., Kim M.J., Kang S.Y., Lee S.H., Kim H.J. *et al.* (2011) Design and synthesis of novel arylpiperazine derivatives containing the imidazole core targeting 5-HT<sub>2A</sub> receptor and 5-HT transporter. *J Med Chem*;54:6305–6318.
  37. Khan M.F., Kumar P., Pandey J., Srivastava A.K., Tamrakar A.K., Maurya R. (2012) Synthesis of novel imbricatolic acid analogues via insertion of N-substituted piperazine at C-15/C-19 positions, displaying glucose uptake stimulation in L6 skeletal muscle cells. *Bioorg Med Chem Lett*;22:4636–4639.
  38. Baki A., Bielik A., Molnar L., Szendrei G., Keseru G.M. (2007) A high throughput luminescent assay for glycogen synthase kinase-3 $\beta$  inhibitors. *Assay Drug Dev Technol*;5:75–83.
  39. Castagne V., Moser P., Roux S., Porsolt R.D. (2010) Rodent models of depression: forced swim and tail suspension behavioral despair tests in rats and mice. *Current protocols in pharmacology/editorial board*, SJ Enna (editor-in-chief) [*et al.*]. Chapter 5: Unit 5 8.
  40. Cross J.B., Thompson D.C., Rai B.K., Baber J.C., Fan K.Y., Hu Y. *et al.* (2009) Comparison of several molecular docking programs: pose prediction and virtual screening accuracy. *J Chem Inf Model*;49:1455–1474.
  41. Sastry G.M., Adzhigirey M., Day T., Annabhimoju R., Sherman W. (2013) Protein and ligand preparation: parameters, protocols, and influence on virtual screening enrichments. *J Comput Aided Mol Des*;27:221–234.
  42. Jorgensen W.L. (2009) Efficient drug lead discovery and optimization. *Acc Chem Res*;42:724–733.
  43. Friesner R.A., Banks J.L., Murphy R.B., Halgren T.A., Klicic J.J., Mainz D.T. *et al.* (2004) Glide: a new approach for rapid, accurate docking and scoring. 1. Method and assessment of docking accuracy. *J Med Chem*;47:1739–1749.
  44. Friesner R.A., Murphy R.B., Repasky M.P., Frye L.L., Greenwood J.R., Halgren T.A. *et al.* (2006) Extra precision glide: docking and scoring incorporating a model of hydrophobic enclosure for protein–ligand complexes. *J Med Chem*;49:6177–6196.
  45. Shafi S., Mahboob Alam M., Mulakayala N., Mulakayala C., Vanaja G., Kalle A.M. *et al.* (2012) Synthesis of novel 2-mercapto benzothiazole and 1,2,3-triazole based bis-heterocycles: their anti-inflammatory and anti-nociceptive activities. *Eur J Med Chem*;49:324–333.
  46. Xcalibur CCD System. (2007) Abingdon, Oxfordshire, England: Oxford Diffraction Ltd.
  47. Clark R.C., Reid J.S. (1995) The analytical calculation of absorption in multifaceted crystals. *Acta Crystallogr A*;51:887–897.
  48. Sheldrick G.M. (2008) A short history of SHELX. *Acta Crystallogr A*;64:112–122.

## Supporting Information

Additional Supporting Information may be found in the online version of this article:

**Table S1.** Structural data and GSK-3 inhibitory activity of piperazinyl pyrimidin-4-one.

**Table S2.** Structural data and GSK-3 $\beta$  inhibitory activity of piperazinyl pyrimidin-4-one.

**Table S3.** Glide extra precision (XP) G-score and number of hydrogen bonds of top-ranked docked ligands and Prime MMGBSA.